Section: Radiodiagnosis

Original Research Article

MRI IN PRIMARY BONE TUMOURS OF THE APPENDICULAR SKELETON: A PROSPECTIVE STUDY WITH HISTOPATHOLOGICAL CORRELATION

Shyamala Javvadi[1], CH Anusha[2], Chalasani Kiranmayi[3]

[1]*MBBS MD, Radiology, Department of Radiodiagnosis, Arundathi Institute of Medical Sciences, Hyderabad, Telangana, India.*
[2]*MBBS MD Radiology, Department of Radiodiagnosis, Arundathi Institute of Medical Sciences, Hyderabad, Telangana, India.*
[3]*MBBS, MD Radiology, Department of Radiodiagnosis, Sprint Diagnostics, Hyderabad, Telangana, India.*

Received *: 20/03/2026*
Received in revised form *: 01/05/2026*
Accepted *: 16/05/2026*

Corresponding Author:
Dr. Chalasani Kiranmayi,
MBBS, MD Radiology, Department of Radiodiagnosis, Sprint Diagnostics, Hyderabad, Telangana, India.
Email: kiranmayi.chalasani@gmail.com

DOI: 10.70034/ijmedph.2026.2.448

Source of Support: Nil,
Conflict of Interest: None declared

Int J Med Pub Health
2026; 16 (2); 2710-2716

ABSTRACT

Background: Primary bone tumours of the appendicular skeleton encompass a heterogeneous group of lesions arising from diverse cell types. Magnetic resonance imaging (MRI) provides multiplanar capability and superior soft tissue contrast, making it the preferred modality for local tumour characterisation and staging after initial radiographic evaluation. **Objectives:** To characterise primary appendicular bone tumours on MRI using T1-weighted, T2-weighted, and STIR sequences; to evaluate MRI-based differentiation of benign from malignant lesions; and to determine the concordance between MRI and histopathological diagnoses in cases where tissue verification was available.
Materials and Methods: A prospective, single-centre, hospital-based study enrolled 30 patients (18 males, 12 females; age range 7–65 years; mean 30.1 years) with suspected or confirmed primary bone tumours of the appendicular skeleton over two years (2017–2019). All patients underwent digital plain radiography followed by MRI at 1.5 Tesla. Histopathological verification was obtained in 22 of 30 cases.
Results: Of 30 cases, 25 (83.3%) were benign and 5 (16.7%) were malignant on MRI. Enchondroma was the most frequent tumour on MRI (n=5, 16.7%); giant cell tumour was the most common on histopathology (n=5, 22.7%). The femur was the most commonly involved bone (n=8, 26.7%). A wide zone of transition was found exclusively in all five malignant cases; all 25 benign cases had a narrow zone of transition. Well-defined margins were significantly more prevalent among benign tumours (chi-square=5.25; p=0.022). All 30 lesions were hyperintense on STIR. MRI concorded with histopathological diagnosis in 20 of 22 verified cases (90.9%).
Conclusions: MRI demonstrated 90.9% concordance with histopathological diagnosis in the verified subset and effectively delineated tumour extent across imaging planes. The zone of transition provided the most consistent separation between benign and malignant lesions in this dataset. Histopathological confirmation remains essential when imaging features are equivocal or in atypical anatomical locations.
Keywords: Magnetic resonance imaging; bone neoplasms; appendicular skeleton; histopathological correlation; musculoskeletal tumours.

INTRODUCTION

Primary bone tumours are uncommon but clinically significant neoplasms. Bone sarcomas account for approximately 0.2% of all malignancies when haematological tumours are excluded, and the age-adjusted incidence for all bone and joint malignancies is in the region of 0.9 per 100,000 persons per year.[1] Their clinical impact is disproportionate to their absolute frequency because they predominantly affect young patients in the first three decades of life, and because their management frequently requires complex surgical planning.[2]

The diagnostic evaluation of any suspected bone lesion begins with plain radiography. Plain films allow efficient assessment of lesion location, matrix mineralisation, cortical architecture, periosteal reaction, and the zone of transition at the tumour–host interface.[3] These features, interpreted alongside the patient's age and clinical context, generate the differential diagnosis that directs further workup. However, radiography does not reliably demonstrate intramedullary extent, soft tissue spread, or the precise spatial relationship of the lesion to adjacent neurovascular structures — information essential for surgical planning.[4,5]

MRI addresses these limitations. Its multiplanar capability and superior contrast resolution between marrow, tumour, and adjacent soft tissues make it the established modality for local tumour staging.[4,5] The STIR sequence effectively suppresses the high signal of normal fatty marrow, enabling clear depiction of intramedullary tumour extent.[6] Fat-saturated post-contrast T1-weighted imaging has been shown to be superior to T2-weighted imaging for demonstrating neurovascular proximity.[7] Specific signal features — including tumour heterogeneity on T2-weighted images, irregular margins, and absence of intratumoral fat — have been examined as potential indicators of malignant biological behaviour.[8,9,10] In a prospective evaluation, sensitivity of 95% and specificity of 84% have been reported for MRI in predicting musculoskeletal tumour malignancy.[11] Nevertheless, tissue sampling remains required for definitive histological classification in most cases.

Data from prospective hospital-based series at teaching institutions in South Asia, where referral patterns differ from specialist bone tumour centres, remain limited. The present study was conducted at a teaching hospital in coastal Andhra Pradesh to prospectively evaluate the role of MRI in characterising primary bone tumours of the appendicular skeleton.

The specific objectives were: (1) to evaluate the role of MRI in detection and characterisation of primary appendicular bone tumours; (2) to assess MRI features differentiating benign from malignant lesions; and (3) to determine concordance between MRI and histopathological diagnoses in verified cases.

MATERIALS AND METHODS

Study design and setting

This was a prospective, hospital-based observational study conducted from January 2017 to December 2019 in the Department of Radiodiagnosis, Konaseema Institute of Medical Sciences and Research Foundation, Amalapuram. Patients were enrolled consecutively as referred from the orthopaedic outpatient department or identified incidentally during imaging for other indications.

Sample size: Sample size was calculated using the formula $n = z^2pq/d^2$, assuming osteosarcoma prevalence of 15% based on a prior institutional series,22 a 95% confidence interval ($z = 1.96$), and absolute precision of 13%, yielding a minimum of 28.9 patients, rounded to 30.

Participants

Eligible patients included those referred for MRI with clinically suspected bone tumours; patients in whom a bone tumour was suspected on prior plain radiography or CT; and patients with incidentally detected bone lesions during imaging for other indications.

Exclusion criteria comprised: ferromagnetic cardiac pacemakers or prosthetic cardiac valves; metallic implants; claustrophobia; inability to maintain supine positioning; non-cooperation; documented adverse reaction to contrast agents; and refusal of written informed consent.

MRI protocol

All imaging was performed on a 1.5 Tesla Philips Achieva scanner with a 16-channel body coil. Patients were positioned supine with the region of interest immobilised. The standard protocol comprised axial T1-weighted and T2-weighted spin echo sequences, STIR, coronal T2-weighted, and sagittal T1-weighted images acquired in three planes. Where clinically indicated, intravenous gadolinium-DTPA was administered at 0.5 mmol/kg body weight and post-contrast T1-weighted images were obtained. Digital plain radiographs in at least two planes preceded MRI in all patients.

Image Analysis

Images were evaluated for: tumour location within the skeleton and within the individual bone; intraosseous site (epiphyseal, metaphyseal, diaphyseal, or combined regions); margin definition (well-defined or ill-defined); zone of transition at the tumour–host interface (narrow or wide); signal intensity on each sequence; internal architecture including septations and fluid-fluid levels; cortical integrity; intramedullary extent; intra-articular extension; neurovascular proximity; and the presence of an associated soft tissue mass.

Reference standard and follow-up

Histopathological examination of surgical or biopsy specimens served as the reference standard for concordance analysis. Of 30 patients, 22 underwent surgery or biopsy and had histopathologically confirmed diagnoses. The remaining eight patients — all with imaging appearances consistent with benign fibrous lesions (fibrous dysplasia n=4, fibrous cortical defect n=2, non-ossifying fibroma n=2) — were managed conservatively on combined radiographic and MRI diagnoses and did not undergo tissue sampling.

Statistical Analysis

Descriptive data are presented as frequencies, percentages, and mean ± standard deviation. The chi-square test was used to assess the association between categorical imaging features and tumour classification (benign versus malignant). Statistical significance was defined as $p < 0.05$. Analyses were

performed using SPSS version 21.0 and Microsoft Excel 2013.

Ethics and informed consent

The study was conducted under institutional ethics committee oversight. Written informed consent was obtained from all participants or their legal representatives prior to enrolment. Individual participant identities were not disclosed in any published output.

RESULTS

Demographic and clinical profile

Thirty patients were enrolled. Ages ranged from 7 to 65 years (mean 30.1 years). Males comprised 18 patients (60.0%) and females 12 (40.0%), yielding a male-to-female ratio of 3:2. The 11–20 year age group was the most frequently represented (n=8, 26.7%), followed by the 41–50 year group (n=7, 23.3%) and the 21–30 year group (n=6, 20.0%). Four patients were aged 31–40 years, three were below 10 years, and one each fell in the 51–60 and 61–70 year groups. [Table 1]

Table 1: Clinicodemographic profile and tumour type distribution on MRI (n = 30)

Variable	Category	n (%)
Sex	Male	18 (60.0)
	Female	12 (40.0)
Age group (years)	≤10	3 (10.0)
	11–20	8 (26.7)
	21–30	6 (20.0)
	31–40	4 (13.3)
	41–50	7 (23.3)
	51–60	1 (3.3)
	61–70	1 (3.3)
Tumour classification (MRI)	Benign	25 (83.3)
	Malignant	5 (16.7)
Tumour type on MRI	Enchondroma	5 (16.7)
	Giant cell tumour	4 (13.3)
	Fibrous dysplasia	4 (13.3)
	Osteochondroma	3 (10.0)
	Osteosarcoma	3 (10.0)
	Aneurysmal bone cyst	2 (6.7)
	Chondromyxoid fibroma	2 (6.7)
	Multiple myeloma	2 (6.7)
	Non-ossifying fibroma	2 (6.7)
	Fibrous cortical defect	2 (6.7)
	Simple bone cyst	1 (3.3)
Bone involved	Femur	8 (26.7)
	Tibia	7 (23.3)
	Phalanges	4 (13.3)
	Pelvic bones	4 (13.3)
	Humerus	3 (10.0)
	Fibula	2 (6.7)
	Metacarpal	1 (3.3)
	Tarsal bone	1 (3.3)

Three cases had multi-bone involvement (2 multiple myeloma, 1 fibrous dysplasia); each bone counted separately in bone-involved rows. Tumour type and bone-involved totals = 30.

Tumour type distribution on MRI

Of 30 cases, 25 (83.3%) were classified as benign and 5 (16.7%) as malignant on MRI. Enchondroma was the most frequently identified tumour (n=5, 16.7%). Giant cell tumour (GCT) and fibrous dysplasia each accounted for 4 cases (13.3%). Osteochondroma and osteosarcoma were identified in 3 cases each (10.0%). Aneurysmal bone cyst, chondromyxoid fibroma, multiple myeloma, non-ossifying fibroma, and fibrous cortical defect each comprised 2 cases (6.7%). A single case of simple bone cyst was recorded (3.3%).

Figure 1. Case Enrollment and Histopathological Verification Flowchart

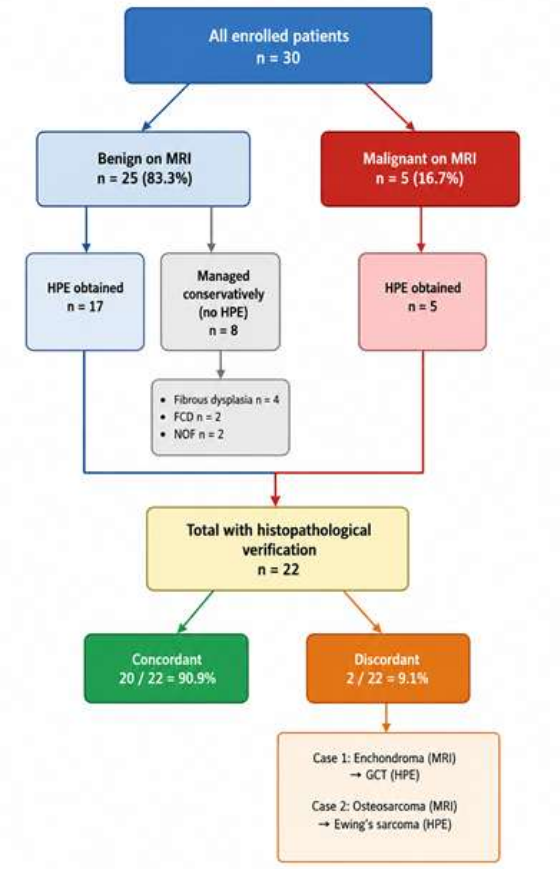

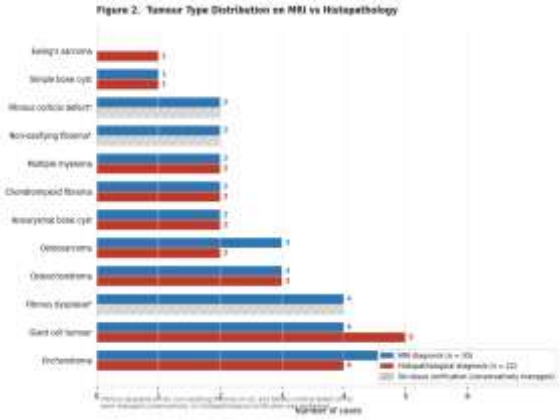

Anatomical location

The femur was the most commonly affected bone (n=8, 26.7%), followed by the tibia (n=7, 23.3%), phalanges (n=4, 13.3%), and pelvic bones (n=4, 13.3%). The humerus was involved in 3 cases (10.0%) and the fibula in 2 cases (6.7%). Three cases involved more than one bone — 2 cases of multiple myeloma and 1 polyostotic fibrous dysplasia case.

Intraosseous site analysis was performed for the 27 single-bone cases, excluding 3 multi-bone cases. The diaphyseal region was the most frequent site (n=11, 40.7%), followed by the meta-diaphyseal region (n=10, 37.0%). The metaphyseal, epi-metaphyseal, and epiphyso-meta-diaphyseal regions each accounted for 2 cases (7.4%).

MRI signal intensity findings

On T1-weighted images, 17 lesions (56.7%) were hypointense, 12 (40.0%) isointense, and 1 (3.3%) hyperintense. The sole T1-hyperintense lesion was a GCT involving the talus. On T2-weighted sequences, 26 lesions (86.7%) were hyperintense and 2 (6.7%) hypointense; these 2 hypointense lesions corresponded to 1 case of multiple myeloma and 1 case of fibrous cortical defect. All 30 lesions (100%) were hyperintense on STIR sequences. Internal septations or trabeculations were identified in 9 cases (30.0%), occurring in GCT (n=4), aneurysmal bone cyst (n=2), fibrous dysplasia (n=2), and non-ossifying fibroma (n=1).

Margins, zone of transition, and soft tissue involvement

Well-defined lesion margins were present in 28 of 30 cases (93.3%); 25 were benign and 3 were malignant. The 3 malignant cases with well-defined margins were 2 multiple myeloma lesions and 1 parosteal osteosarcoma. The 2 cases with ill-defined margins (6.7%) were both malignant. The difference in margin definition between groups was statistically significant (chi-square=5.25; p=0.022). [Table 2].

A wide zone of transition was present exclusively in all 5 malignant cases, while all 25 benign cases had a narrow zone of transition — constituting complete group separation on this parameter. [Table 2]

Table 2: MRI imaging features compared between benign and malignant tumours (n = 30)

MRI Feature	Benign (n=25) n (%)	Malignant (n=5) n (%)	Total (n=30) n (%)	p-value
Margins				
Well-defined	25 (100.0)	3 (60.0)	28 (93.3)	0.022*
Ill-defined	0 (0.0)	2 (40.0)	2 (6.7)	
Zone of transition				
Narrow	25 (100.0)	0 (0.0)	25 (83.3)	—†
Wide	0 (0.0)	5 (100.0)	5 (16.7)	
T1 signal intensity				
Hypointense	14 (56.0)	3 (60.0)	17 (56.7)	NR
Isointense	10 (40.0)	2 (40.0)	12 (40.0)	NR
Hyperintense	1 (4.0)	0 (0.0)	1 (3.3)	NR
STIR signal				
Hyperintense (all)	25 (100.0)	5 (100.0)	30 (100.0)	NR
Soft tissue involvement	10 (40.0)	5 (100.0)	15 (50.0)	NR
Internal septations	9 (36.0)	0 (0.0)	9 (30.0)	NR

**Chi-square = 5.25; p = 0.022. †Complete group separation observed; formal chi-square not computed in source. NR = formal statistical test not reported for this variable.*

Periosteal reaction was identified in all 3 osteosarcoma cases. Soft tissue involvement was documented in 15 cases (50.0%): all 5 malignant cases and 10 of 25 benign cases.

Histopathological findings and MRI–histopathology concordance

Histopathological verification was available for 22 of 30 patients. On histopathology, GCT was the most frequently confirmed diagnosis (n=5, 22.7%), followed by enchondroma (n=4, 18.2%), osteochondroma (n=3, 13.6%), osteosarcoma (n=2, 9.1%), multiple myeloma (n=2, 9.1%), aneurysmal bone cyst (n=2, 9.1%), and chondromyxoid fibroma (n=2, 9.1%). Simple bone cyst and Ewing's sarcoma each accounted for 1 case (4.5%).

MRI was concordant with histopathological diagnosis in 20 of 22 verified cases, giving a concordance rate of 90.9% within the verified subset.

Table 3: MRI diagnosis versus histopathological diagnosis in verified cases (n = 22)

MRI Diagnosis	Histopathological Diagnosis	Concordance	n
Giant cell tumour	Giant cell tumour	Yes	4
Enchondroma	Giant cell tumour	NO	1
Enchondroma	Enchondroma	Yes	4
Osteochondroma	Osteochondroma	Yes	3
Aneurysmal bone cyst	Aneurysmal bone cyst	Yes	2
Chondromyxoid fibroma	Chondromyxoid fibroma	Yes	2
Simple bone cyst	Simple bone cyst	Yes	1
Osteosarcoma	Osteosarcoma	Yes	2
Osteosarcoma	Ewing's sarcoma	NO	1
Multiple myeloma	Multiple myeloma	Yes	2
TOTAL	**20 concordant / 2 discordant**	**90.9%**	**22**

Concordance rate in histopathologically verified subset: 20/22 = 90.9%. Discordant rows highlighted. Eight conservatively managed cases (fibrous dysplasia n=4; fibrous cortical defect n=2; non-ossifying fibroma n=2) not included — no tissue confirmation obtained.

Two cases were discordant. In the first, a phalanx lesion showing T1 hypointensity, T2/STIR hyperintensity, internal septations, and cortical breach was attributed to enchondroma on MRI but confirmed as GCT on histopathology. In the second, a femoral meta-diaphyseal lesion with wide zone of transition, ill-defined margins, and periosteal reaction was attributed to osteosarcoma on MRI; histopathology confirmed Ewing's sarcoma.

DISCUSSION

This prospective study evaluated 30 patients with primary appendicular bone tumours using a standardised multisequence MRI protocol, with histopathological confirmation in 22 cases.

Age, sex, and demographic distribution

The second decade of life was the most represented age group in this series, consistent with the documented bimodal incidence pattern of bone sarcomas — with an early peak in the second decade during maximal skeletal growth.1 Published Indian institutional series report similar clustering: Baweja et al. found the 10–20 year group to be the most common in their 25-patient MRI-based series (mean age 24.64 years), and Goud et al. similarly identified the 11–20 year group as most frequently represented in their 53-patient prospective study.[12,22] The male predominance of 60.0% in the present series aligns with these reports.[12,22]

Tumour spectrum and benign-to-malignant ratio

The high proportion of benign cases (83.3%) differs from selected published series. Baweja et al. recorded 80% malignant tumours in 25 patients, while Goud et al. found 45% malignant lesions.[12,22] This difference most plausibly reflects the inclusive prospective enrolment strategy in the present study, drawing on a mixed general orthopaedic outpatient base — including suspected, confirmed, and incidentally identified lesions — rather than restricting enrolment to histologically confirmed or high-suspicion malignant cases.

Enchondroma was the most frequent tumour on MRI (16.7%), predominantly in the short tubular bones of the hand — the classic anatomical predilection for this entity.[16,17] On histopathology, however, GCT emerged as the most common diagnosis (22.7%), partly because one phalanx lesion attributed to enchondroma on MRI was reclassified as GCT at tissue sampling, illustrating the morphological overlap between these entities in atypical locations.

Giant cell tumour

GCT was identified in 4 cases on MRI and confirmed in 5 on histopathology. All MRI-identified GCT cases presented as expansile lytic lesions with internal septations, consistent with the established imaging profile for this entity.13,14 Multiplanar MRI enabled identification of intra-articular extension in 3 of 4 GCT cases — a clinically important finding given that stage 3 GCT characteristically transgresses natural barriers. The single GCT demonstrating T1 signal hyperintensity — located in the talus — likely reflects haemorrhagic or proteinaceous intratumoral content, occasionally described for this tumour type.[14]

Signal intensity characteristics and STIR sensitivity

T1 hypointensity was the predominant pattern (56.7%), consistent with the solid or fibrous composition characteristic of most tumour types in this series. Universal STIR hyperintensity across all 30 cases confirms the high sensitivity of fat-suppressed fluid-sensitive sequences for lesion detection, consistent with prior evidence.6 However, STIR could not differentiate benign from malignant lesions in this dataset and is best employed as a

detection tool in combination with T1-weighted and T2-weighted evaluation. T2 heterogeneity was present across both benign and malignant cases, consistent with earlier reports that inhomogeneous T2 signal alone should not be used as a reliable indicator of malignant biological behaviour.[9]

T2 hypointensity in 2 cases — one multiple myeloma and one fibrous cortical defect — reflects the dense cellularity and fibrous tissue content of these entities respectively, both of which restrict water proton mobility relative to the fluid-equivalent signal seen in cartilaginous and cystic lesions.[8,10]

Zone of transition and margin definition

The zone of transition provided complete group separation in this dataset: all 5 malignant lesions had a wide zone of transition and all 25 benign lesions had a narrow zone. This finding is qualitatively consistent with the observations of Goud et al., who found a wide zone exclusively in malignant cases, and Baweja et al., who found a wide zone in 16 of 20 malignant cases.[12,22] The complete separation here should be interpreted with caution given the small malignant cohort of 5 cases; the zone of transition should be integrated with other radiological and clinical findings rather than applied as a standalone test.

Margin definition also differed significantly ($p=0.022$), but 3 malignant tumours — 2 multiple myeloma cases and 1 parosteal osteosarcoma — had well-defined margins, demonstrating that margin definition alone cannot exclude malignancy across all tumour types, as noted in published comparison series.[12,22]

Osteosarcoma

Three osteosarcoma cases were identified on MRI, all in male patients aged 25–38 years, located in the femur, tibia, and humerus. All three showed wide zones of transition and periosteal reaction. The parosteal osteosarcoma — a low-grade juxtacortical variant — arose from the diaphysis of the humerus and demonstrated the characteristic lobulated exophytic morphology with defined margins and cortical surface origin described for this subtype.[20,21] MRI effectively delineated soft tissue extent and cortical involvement in all three cases. Of the three, one was reclassified as Ewing's sarcoma on histopathology, forming one of the two discordant cases.

Aneurysmal bone cyst

Both ABC cases were in the second decade of life and presented as expansile multicystic lytic lesions with septal enhancement and T2/STIR hyperintensity, consistent with published descriptions.18 Fluid-fluid levels reflecting layering of blood products were identified in one of the two cases; these have been documented in 20–100% of ABC cases in prior series.[19]

Discordant cases and diagnostic limitations

Two discordant cases illustrate specific pitfalls of MRI-based diagnosis. The enchondroma-GCT discordance arose in a phalanx of the hand — an atypical location for GCT, where the characteristic subarticular lytic appearance seen at the distal femur and proximal tibia may not be present. In small, short tubular bones, reliable differentiation between GCT and enchondroma on imaging alone is unreliable.[13,16] The osteosarcoma-Ewing's sarcoma discordance reflects the well-recognised imaging overlap between these tumours, which share aggressive features — wide zone of transition, cortical destruction, periosteal reaction, and soft tissue extension — that cannot be differentiated on MRI morphology alone. Immunohistochemical analysis is required for their definitive separation.[12]

MRI–histopathology concordance

The 90.9% concordance rate in the 22 verified cases is the primary diagnostic outcome and must be understood within its denominator. Eight conservatively managed benign fibrous lesion cases are not included in this figure. This rate broadly aligns with published reports including Baweja et al.[12] Direct numerical comparison across institutions is limited by differences in sample composition, tumour spectrum, and proportion of verified cases, but the finding is consistent with the general evidence base that MRI with standard multisequence protocols provides reliable characterisation for most primary appendicular bone tumours.

Limitations

Several limitations should be considered. The total sample of 30 patients is small; the malignant subgroup comprised only 5 cases, precluding formal computation of sensitivity, specificity, and predictive values for individual MRI features. This single-centre study enrolled patients from a general orthopaedic outpatient base; the tumour spectrum and benign-to-malignant ratio may not reflect those at specialist musculoskeletal oncology centres. Histopathological verification was not obtained for 8 of 30 patients; the concordance rate of 90.9% applies solely to the 22 verified cases. Statistical analysis was restricted to descriptive statistics and chi-square testing for two categorical variables, without multivariate modelling or diagnostic accuracy analysis. Advanced quantitative MRI methods — diffusion-weighted imaging and dynamic contrast-enhanced MRI — were not employed, limiting comparability with more recent quantitative series. Inter-observer agreement was not assessed. Minor arithmetical discrepancies identified in the source data have been reconciled; authors should verify all figures against the original case records before submission.

CONCLUSION

In this prospective single-centre study of 30 patients with primary appendicular bone tumours, MRI achieved diagnostic concordance with histopathological diagnosis in 90.9% of the 22 histopathologically verified cases. The zone of transition provided complete separation between benign and malignant lesions in this dataset, and well-defined lesion margins were significantly more

prevalent in the benign group (p=0.022). STIR hyperintensity was universal across all lesion types, confirming the sensitivity of fat-suppressed sequences for detection but not for characterisation. MRI contributed clinically relevant information regarding tumour extent, cortical involvement, intra-articular extension, and soft tissue spread across the spectrum of lesions studied. Two discordant cases — one GCT misclassified as enchondroma in the hand and one Ewing's sarcoma misclassified as osteosarcoma — underline the irreplaceable role of histopathological confirmation when imaging morphology is atypical, location is unusual, or tumour types with overlapping features are being considered.

REFERENCES

1. Franchi A. Epidemiology and classification of bone tumors. Clinical Cases in Mineral and Bone Metabolism. 2012;9(2):92–5.
2. Nomikos GC, Murphey MD, Kransdorf MJ, Bancroft LW, Peterson JJ. Primary bone tumors of the lower extremities. Radiologic Clinics of North America. 2002;40(5):971–90.
3. Costelloe CM, Madewell JE. Radiography in the initial diagnosis of primary bone tumors. American Journal of Roentgenology. 2013;200(1):3–7.
4. Ehara S. MR imaging in staging of bone tumors. Cancer Imaging. 2006;6(1):158–62.
5. Stacy GS, Mahal RS, Peabody TD. Staging of bone tumors: a review with illustrative examples. American Journal of Roentgenology. 2006;186(4):967–76.
6. Golfieri R, Baddeley H, Pringle JS, Souhami R. The role of the STIR sequence in magnetic resonance imaging examination of bone tumours. British Journal of Radiology. 1990;63(748):251–6.
7. Gronemeyer SA, Kauffman WM, Rocha MS, Steen RG, Fletcher BD. Fat-saturated contrast-enhanced T1-weighted MRI in evaluation of osteosarcoma and Ewing sarcoma. Journal of Magnetic Resonance Imaging. 1997;7(3):585–9.
8. De Schepper AM, De Beuckeleer L, Vandevenne J, Somville J. Magnetic resonance imaging of soft tissue tumors. European Radiology. 2000;10(2):213–23.
9. Pang KK, Hughes T. MR imaging of the musculoskeletal soft tissue mass: is heterogeneity a sign of malignancy? Journal of the Chinese Medical Association. 2003;66(11):655–61.
10. Simpfendorfer CS, Ilaslan H, Davies AM, James SL, Obuchowski NA, Sundaram M. Does the presence of focal normal marrow fat signal within a tumor on MRI exclude malignancy? An analysis of 184 histologically proven tumors of the pelvic and appendicular skeleton. Skeletal Radiology. 2008;37(9):797–804.
11. Daniel A, Ullah E, Wahab S, Kumar V. Relevance of MRI in prediction of malignancy of musculoskeletal system — a prospective evaluation. BMC Musculoskeletal Disorders. 2009;10(1):125.
12. Baweja S, Arora R, Singh S, Sharma A, Narang P, Ghuman S, et al. Evaluation of bone tumors with magnetic resonance imaging and correlation with surgical and gross pathological findings. Indian Journal of Radiology and Imaging. 2006;16(4):611–8.
13. Murphey MD, Nomikos GC, Flemming DJ, Gannon FH, Temple HT, Kransdorf MJ. Imaging of giant cell tumor and giant cell reparative granuloma of bone: radiologic-pathologic correlation. RadioGraphics. 2001;21(5):1283–309.
14. Turcotte RE. Giant cell tumor of bone. Orthopedic Clinics of North America. 2006;37(1):35–51.
15. Bloem JL, Van der Woude HJ, Geirnaerdt M, Hogendoorn PC, Taminiau AH, Hermans J. Does magnetic resonance imaging make a difference for patients with musculoskeletal sarcoma? British Journal of Radiology. 1997;70(832):327–37.
16. Aoki J, Sone S, Fujioka F, Terayama K, Ishii K, Karakida O, et al. MR of enchondroma and chondrosarcoma: rings and arcs of Gd-DTPA enhancement. Journal of Computer Assisted Tomography. 1991;15(6):1011–6.
17. Cohen EK, Kressel HY, Frank TS, Fallon M, Kressel MA, Dalinka MK, et al. Hyaline cartilage-origin bone and soft-tissue neoplasms: MR appearance and histologic correlation. Radiology. 1988;167(2):477–81.
18. Kransdorf MJ, Sweet DE. Aneurysmal bone cyst: concept, controversy, clinical presentation, and imaging. American Journal of Roentgenology. 1995;164(3):573–80.
19. Van Dyck P, Vanhoenacker FM, Vogel J, Venstermans C, Kroon HM, Gielen J, et al. Prevalence, extension, and characteristics of fluid-fluid levels in bone and soft tissue tumors. European Radiology. 2006;16(12):2644–51.
20. Jelinek JS, Murphey MD, Kransdorf MJ, Shmookler BM, Malawer MM, Hur RC. Parosteal osteosarcoma: value of MR imaging and CT in the prediction of histologic grade. Radiology. 1996;201(3):837–42.
21. Campanacci M, Picci P, Gherlinzoni F, Guerra A, Bertoni F, Neff JR. Parosteal osteosarcoma. Journal of Bone and Joint Surgery (British). 1984;66(3):313–21.
22. Goud GR, Siddesh MB, Navin A, Patil N. How accurate is MRI in characterisation of primary bone tumors — a prospective evaluation. International Journal of Recent Scientific Research. 2017;8(1):15312–20.